Publication VI

Päivi Sievilä, Nikolai Chekurov, and Ilkka Tittonen. 2010. The fabrication of silicon nanostructures by focused-ion-beam implantation and TMAH wet etching. Nanotechnology, volume 21, number 14, 145301, 6 pages.

Nanotechnology **21** (2010) 145301 (6pp) doi:10.1088/0957-4484/21/14/145301

The fabrication of silicon nanostructures by focused-ion-beam implantation and TMAH wet etching

Päivi Sievilä, Nikolai Chekurov and Ilkka Tittonen

Department of Micro and Nanosciences, Helsinki University of Technology, PO Box 3500, FI-02015 TKK, Finland

E-mail: paivi.sievila@tkk.fi

Received 4 December 2009, in final form 29 January 2010
Published 10 March 2010
Online at stacks.iop.org/Nano/21/145301

Abstract
Local gallium implantation of silicon by a focused ion beam (FIB) has been used to create a mask for anisotropic tetramethylammonium hydroxide (TMAH) wet etching. The dependence of the etch stop properties of gallium-doped silicon on the implanted dose has been investigated and a dose of 4×10^{13} ions cm^{-2} has been determined to be the threshold value for achieving observable etching resistance. Only a thin, approx. 50 nm, surface layer is found to be durable enough to serve as a mask with a high selectivity of at least 2000:1 between implanted and non-implanted areas. The combined FIB–TMAH process has been used to generate various types of 3D nanostructures including nanochannels separated by thin vertical sidewalls with aspect ratios up to 1:30, ultra-narrow (approx. 25 nm) freestanding bridges and cantilevers, and gratings with a resolution of 20 lines μm^{-1}.

1. Introduction

The etch stop effect in boron-doped p$^+$ silicon is one of the fundamental phenomena widely studied and applied in micro- and nanosystems fabrication [1]. A similar effect can be obtained by using gallium, also a p-type dopant, for masking purposes. Focused-ion-beam (FIB) technology enables the fabrication of a wide variety of micro- and nanostructures, and most tools are based on gallium beam machining [2, 3]. Locally Ga$^+$ beam-treated silicon has been utilized in the processing of 3D structures, since the implanted regions have been shown to be selective towards both plasma [4] and wet chemical etching [5–7]. Processes combining gallium implantation with potassium hydroxide (KOH) etching have been carried out and different types of structures including, for example, bridges, beams, nanocups and mirrors have been presented [8–10].

The advantages of TMAH etching are a smooth surface obtained with concentrations exceeding 22 wt% of TMAH ($(CH_3)_4NOH$) in water solution [11] and low toxicity. The most important benefit of TMAH compared with KOH is the compatibility with CMOS processing, since the etch solution does not contain any metallic ions. There is, however, very little data reported on the Ga masking effect in TMAH wet etching compared to that of KOH. Bai *et al* have presented silicon fine structures fabricated by FIB implantation of Si^{2+} ions followed by TMAH etching [12], and Masahara *et al* have shown experimental results concerning As-, P-and BF_2-ion-bombardment-retarded etch rates of Si in 2.38% TMAH [13].

The purpose of this work is to specifically investigate the etch stop behavior of an FIB-implanted gallium mask in anisotropic wet etching of ⟨100⟩ and ⟨110⟩ silicon in 25% TMAH solution, aiming to utilize the results in the fabrication of high perfection nanostructures. The masking capability between Ga$^+$-implanted and non-implanted regions is determined for various ion doses, and the method is, in addition, shown to be suitable for obtaining very deep (over 100 μm) etching profiles. A gallium-implanted mask is used to fabricate high resolution gratings, high aspect ratio nanochannels, and freestanding bridges and cantilevers with a minimum feature size as small as 25 nm.

2. Selectivity experiments

A Helios Nanolab 600 dual-beam system (FEI Company) was used for the local gallium ion implantation. The Ga$^+$ ion beam was generated using a liquid metal source. The current can be varied between 1.5 pA and 22 nA and the dwell time between 50 ns and 4.6 ms.

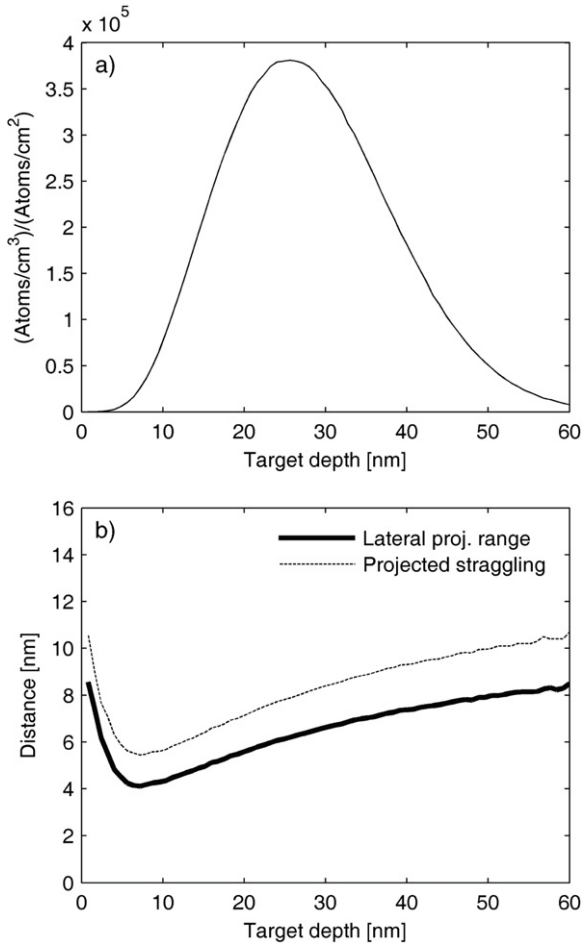

Figure 1. Gallium ion distribution in silicon: (a) ion depth distribution and (b) projected lateral spread of ions. The ion energy is 30 keV.

The Ga^+ ion distribution in silicon was modeled by 'The Stopping and Range of Ions in Matter' (SRIM) [14], an ion impact analysis software program utilizing Monte Carlo simulation. The results are shown in figure 1. The ion energy of 30 keV used in the experiments produces a doped surface layer in silicon whose range is 28 nm with a standard deviation of 10 nm. The depth distribution determines the thickness of the Ga^+ mask. The lateral range is 6 nm with a standard deviation of 8 nm, which together with the shape of the ion beam limits the minimum linewidth of the implanted patterns.

The experiments were performed on ⟨100⟩ silicon wafers with p-type doping and resistivity of 2–3 Ω cm, and ⟨110⟩ silicon wafers with p-type doping and resistivity of 0.02–0.035 Ω cm. Prior to the etching experiments the samples were dipped in buffered hydrofluoric acid (BHF) to remove native oxide (15 s, room temperature).

To investigate the dependence of the etch resistance on the ion dose, a sequence of 600 μm × 600 μm square areas were irradiated with ion doses varying from 2×10^{13} to 4×10^{16} ions cm^{-2}. The samples were etched in 25% aqueous TMAH solution at 85 °C. The etch rate of the (100) Si crystal plane is about 0.6 μm min^{-1} and of the (110) crystal plane about 1.4 μm min^{-1}. The experiment was repeated for ⟨100⟩ silicon at 60 °C, in which case the etch rate is approximately 150 nm min^{-1}. The etching in TMAH was performed for several time periods and the heights of the resulting structures were measured with a profilometer. During each etching period the height difference between the implanted regions and the surrounding Si surface increases until the doped layer is totally etched away. This maximum achievable height for each dose remains approximately constant during the subsequent etching steps. The accuracy of the height values is limited by Si surface roughening around the implanted areas during TMAH etching. The average standard deviation of the measured heights is around 4% of the given values, excluding the lowest data points with higher uncertainty (dose below 5×10^{13} ions cm^{-2}). The principle of fabrication is shown in figure 2.

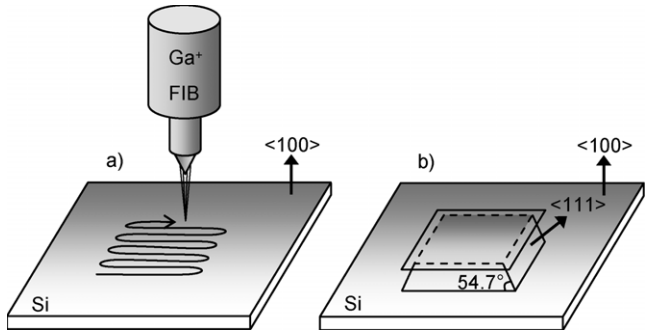

Figure 2. Schematic fabrication process: (a) local FIB implantation of patterns and (b) resulting structure after TMAH etching.

Figure 3 shows the masking behavior plotted against gallium ion dose. The critical dose producing a noticeable step height (50 nm) can be determined to be 2×10^{13} ions cm^{-2} in this experiment. With a dose exceeding 4×10^{16} ions cm^{-2} the selectivity between treated and untreated silicon is better than 1:2000, when using the approximate value for the thickness of the Ga^+-doped layer of 50 nm. With higher doses, the ion-bombardment-induced sputtering of silicon during the FIB doping will become significant. The obtained selectivity is comparable to the selectivities of SiO_2 and Si_3N_4 masks typically used in TMAH etching of Si [15]. The maximum depth values in figure 3(a) are sensitive to the etching conditions and are merely indicative. It is recommended to exceed the corresponding dose values by at least a factor of two to ensure the mask integrity.

The etch stop mechanism of gallium ion doping of silicon is not truly understood. The amorphization of Si induced by ion irradiation and the decrease of free electrons have been proposed to be responsible for the etch stop phenomenon [13]. Another possible explanation is the formation of non-volatile gallium oxide in the doped surface layer during the etch process, which has been investigated by means of secondary ion mass spectroscopy (SIMS) and x-ray photoelectron spectroscopy (XPS) for both dry and wet chemical etched samples [4, 16].

3. Nanoscale structures

Various types of nanostructures were fabricated in order to characterize the patterning and etching processes with

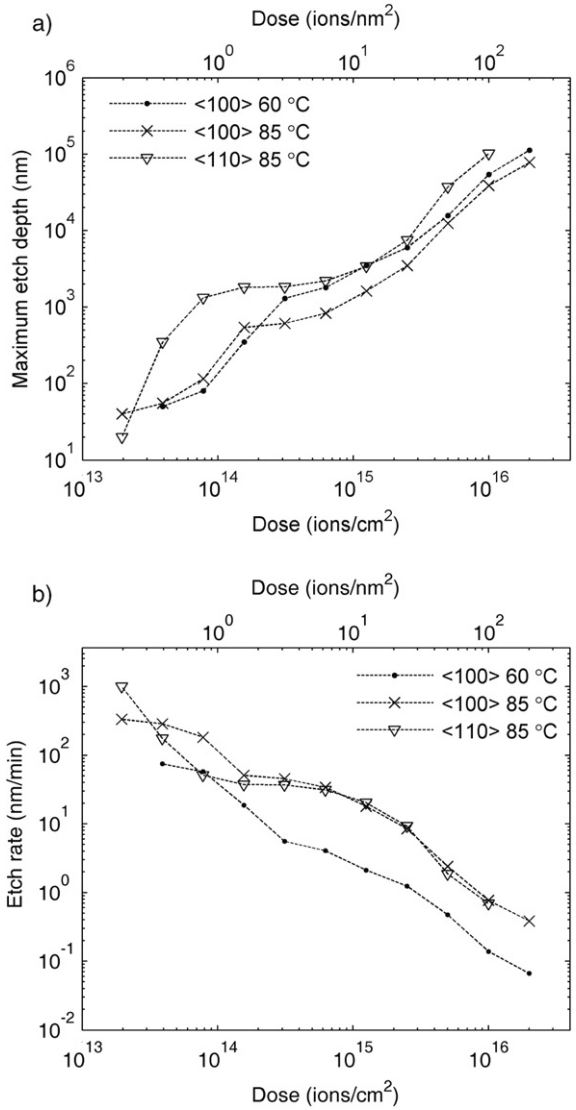

Figure 3. (a) Dependence of the maximum achievable etch depth on the ion dose for ⟨100⟩ Si at 60 and 85 °C and for ⟨110⟩ Si at 85 °C. (b) Corresponding etch rate of Ga^+-doped Si mask. The mask thickness is approximated to be 50 nm. Critical dose for Si amorphization is approx. 10^{14} cm^{-2} [15], which is also indicated by the match of the curves measured at 85 °C.

respective limitations. In these experiments, ⟨100⟩ and ⟨110⟩ wafers with the same specifications as in the etch selectivity tests were used. All the structures were patterned with an ion beam current of 1.5 pA and energy of 30 keV. Again, room temperature BHF was used for native oxide removal before etching.

3.1. Resolution

In order to study the spatial resolution of the process, a sequence of gratings with varying periods was implanted on ⟨100⟩ silicon. The sample was etched for 35 s in 85 °C TMAH solution and the resulting grating profiles were investigated by making cross sections using FIB milling. Figure 4 shows two structures where the lines were exposed with a dose of 10^{15} ions cm^{-2}. The narrowest reproducible line is 40 nm

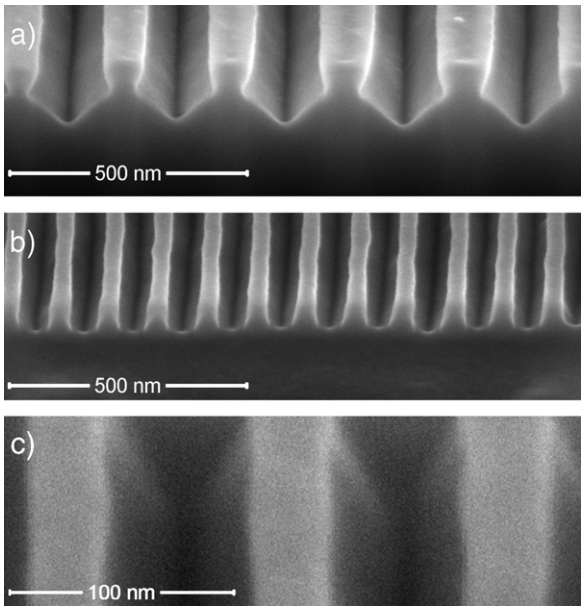

Figure 4. Grating structures on ⟨100⟩ silicon: (a) cross section of a varying period of 210–245 nm, (b) cross section of a constant period of 100 nm and (c) close-up of a 100 nm period. The v-shape of the groove bottoms is typical for anisotropic wet etching. The shapes of the cross sections are slightly influenced by redeposition of silicon during FIB cutting.

in width and trench 60 nm in width (both are 50 nm on a mask), leading to a resolution of the process of 20 lines μm^{-1} (figures 4(b) and (c)). The width of the final structures is affected by the Ga^+ ion dose used for doping and the imperfect anisotropy of TMAH etching.

3.2. Freestanding elements

The thin insoluble masking layer can also be utilized in making freestanding, amorphous Ga^+-doped Si elements. Ultra-narrow cantilevers (figure 5) and bridges (figure 6) were fabricated on ⟨100⟩ Si by aligning the structures 45° off the ⟨110⟩-directed main axes on the substrate. Under these conditions the (100) planes appear in parallel to the direction of the cantilevers, forming 90° fast etching sidewalls and leading to release during etching (85 °C, 25% TMAH, 1 min). No stress-related bending of the released beams was detected. The narrowest freestanding feature is only 25 nm wide.

The surface roughness of the patterns was investigated with an atomic force microscope (AFM) before and after etching in TMAH. The measured root mean square (RMS) roughness was approx. 1 nm, the same order of magnitude as the value of an untreated, polished Si surface.

3.3. Vertical channels on ⟨110⟩ silicon

Single-crystal ⟨110⟩ silicon enables etching of nearly vertical, high surface quality walls. The mask must be aligned so that the slowly etching (111) planes form the sidewalls. Nanochannels separated by very narrow vertical ridges were implanted by aligning the channels perpendicular to the ⟨111⟩ crystal direction. The sample was etched in 85 °C TMAH

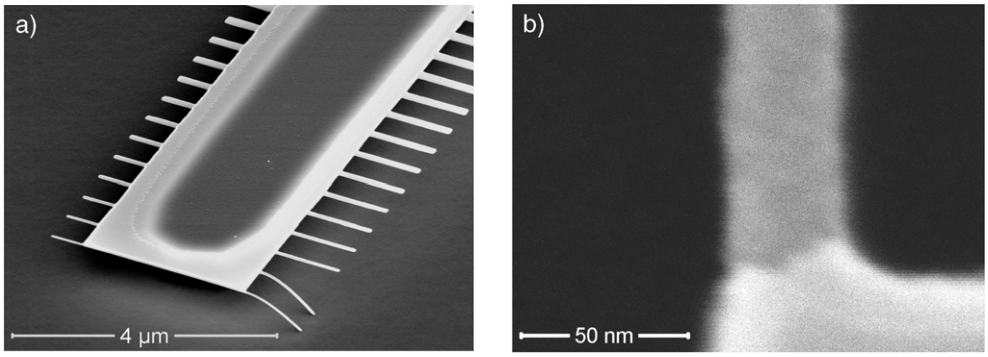

Figure 5. (a) Series of freestanding cantilevers on ⟨100⟩ Si substrate. The implantation dose was 4×10^{15} ions cm^{-2}. The length of the cantilevers is 0.5 μm (left) and 1 μm (right), the thickness approx. 50 nm and the width of the narrowest beams 35 nm. The two bridges adhere to the substrate because of stiction deriving from the drying step of the wet release process. (b) Top view of the narrowest beam.

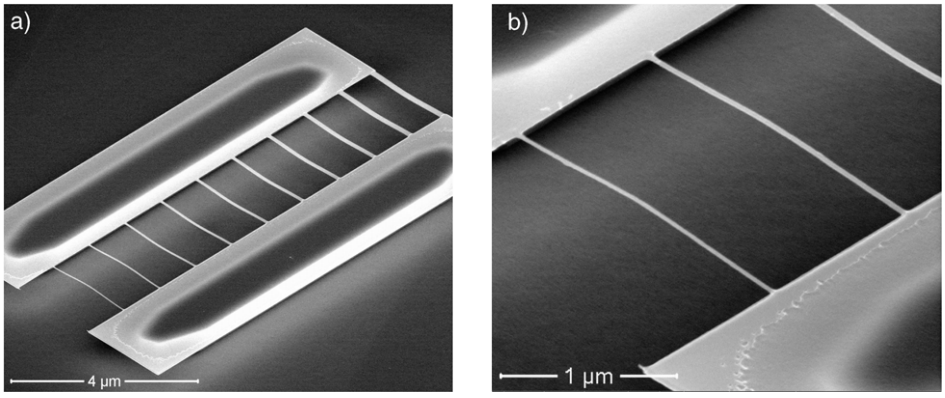

Figure 6. (a) Series of 2 μm long freestanding bridges (dose 2×10^{15} ions cm^{-2}). The widths range from 25 to 145 nm. (b) Close-up view of the narrowest bridges.

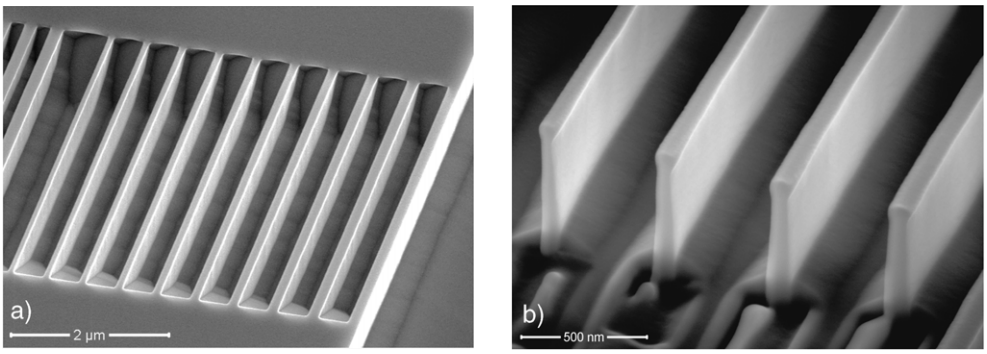

Figure 7. Nanochannels separated by vertical sidewalls on the ⟨110⟩ Si substrate. The gallium dose used for patterning was 2×10^{15} ions cm^{-2}. On the bottom of the channels, the slowly etching planes have begun to appear and form the self-limiting U-grooves typical for anisotropic ⟨110⟩ Si etching.

solution for 1 min. Figure 7 shows 500 nm wide and 600 nm deep channels. Figure 7(b) shows a cross section of the four narrowest walls (widths ranging from 30 to 60 nm) obtained by cutting the structure with FIB. The downwards widening profile of the cross section of the walls is explained by the redeposition of material during milling.

The anisotropy of the etching and high selectivity of the gallium-implanted mask enables fabrication of very high aspect ratio structures. Figure 8 shows a wall with an aspect ratio of more than 1:30. The height is limited by the wall spacing, since the self-limiting U-grooves determine the depth of the structures. If the distance is longer the height can be further increased.

4. Conclusion

Local gallium implantation by focused ion beam enables a maskless and resist-free, flexible patterning technique

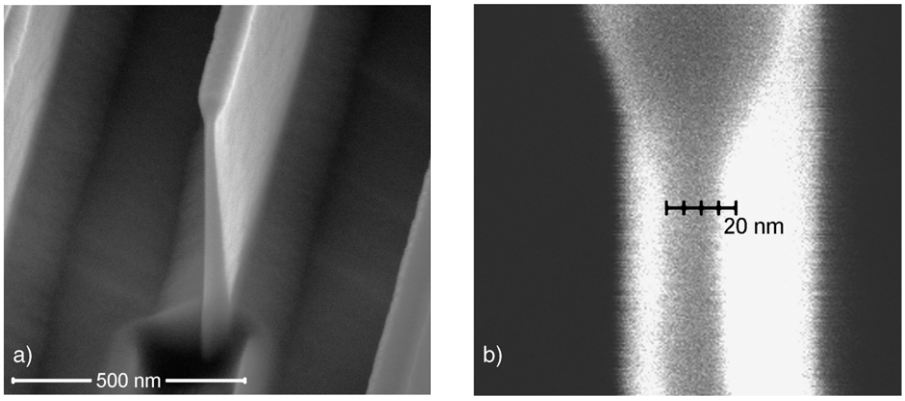

Figure 8. (a) Cross section of a single vertical wall that is 15 nm wide and 570 nm high. The approx. 50 nm thick and 70 nm wide Ga^+-doped masking layer can be seen on the top of the wall (dose 10^{15} ions cm^{-2}). The FIB cutting causes redeposition of silicon that can be seen as a widening of the lowest part of the wall close to the cross section. The valley and ridges in front of the cross section derive from the FIB cutting of the single wall. (b) Perpendicular close-up view of the cross section showing the wall width.

of arbitrary shaped nanostructures. We have shown that an FIB-implanted Ga^+ layer acts as a mask with a high selectivity in TMAH wet etching enabling the fabrication of high resolution gratings, extremely narrow, long and thin freestanding elements, and vertical walls with very high aspect ratio.

The fabrication process shown here is a fast and straightforward method for making prototypes of nanostructures for various purposes, even on samples that need to be processed together with semiconductor circuits. Compared with the direct FIB milling of 3D structures, the described process only modifies a thin surface layer so the writing speed is improved by several orders of magnitude. The typical TMAH etching step in nanostructure fabrication takes only a few minutes, and even tens of Si wafers can be etched at the same time. Thus the throughput of the method is mainly limited by the time needed for FIB writing. The speed is determined by the ion current used for patterning. As an example, an area of $10 \times 10\ \mu m^2$ containing even tens of presented high resolution structures can be implanted with a typical dose of 2×10^{15} ions cm^{-2} in less than 4 min, when the lowest current 1.5 pA is used. Larger patterns can be implanted with a lower resolution using a high current beam. As an example, an area of $600 \times 600\ \mu m^2$ can be modified into an etch-resistant state in less than a minute using the maximum ion current of 21 nA.

Besides prototyping, the mass production of nanostructures can be envisioned supposing the etched structures to be used for stamp fabrication in nanoimprint lithography. The use of SOI wafers provides more opportunities including released, high precision silicon structures like cantilever sensors, mirrors, membranes and switches. The technique is also promising for integrated optics fabrication, prospective components including, for example, gratings, waveguides, photonic crystals and optical resonators. The possibility to generate subwavelength features opens up visions for novel types of light manipulation and plasmonic circuit fabrication.

There are a few feasible improvements in the process that leave space for further investigation. The thickness of the gallium-doped mask and the prospective freestanding structures can be modified by varying the ion energy used in the FIB implantation. In addition, the quality of the wet etched surfaces and the selectivity between the different crystal planes can be manipulated by adding to the TMAH solution isopropanol or proper surfactants such as Triton X-100 [17, 18]. Besides the process development, the experiments will be continued for scaling down components such as resonant sensors and micro-opto-mechanical devices. The technique presented in this work is promising for future applications in which micro- and nanomechanical devices need to be integrated on the same chip with CMOS electronics.

Acknowledgments

PS acknowledges The Graduate School in Electronics, Telecommunications and Automation (GETA) in Finland. Professor S Franssila is acknowledged for useful discussions during the project.

References

[1] Seidel H, Csepregi L, Heuberger A and Baumgärtel H 1990 Anisotropic etching of crystalline silicon in alkaline solutions *J. Electrochem. Soc.* **137** 3626–32

[2] Reyntjens S and Puers R 2001 A review of focused ion beam applications in microsystem technology *J. Micromech. Microeng.* **11** 287–300

[3] Tseng A A 2005 Recent developments in nanofabrication using focused ion beams *Small* **1** 924–39

[4] Chekurov N, Grigoras K, Peltonen A, Franssila S and Tittonen I 2009 The fabrication of silicon nanostructures by local gallium implantation and cryogenic deep reactive ion etching *Nanotechnology* **20** 065307

[5] Berry I L and Caviglia A L 1983 High resolution patterning of silicon by selective gallium doping *J. Vac. Sci. Technol.* B **1** 1059–61

[6] Steckl A J, Mogul H C and Mogren S 1992 Localized fabrication of Si nanostructures by focused ion beam implantation *Appl. Phys. Lett.* **60** 1833–5

[7] Kawasegi N, Morita N, Yamada S, Takano N, Oyama T, Ashida K, Taniguchi J and Miyamoto I 2006 Three-dimensional nanofabrication utilizing selective etching of silicon induced by focused ion beam irradiation *JSME Int. J.* C **49** 583–9

[8] Brugger J, Beljakovic G, Despont M, de Rooij N F and Vettiger P 1997 Silicon micro/nanomechanical device fabrication based on focused ion beam surface modification and KOH etching *Microelectron. Eng.* **35** 401–4

[9] Schmidt B, Bischoff L and Teichert J 1997 Writing FIB implantation and subsequent anisotropic wet chemical etching for fabrication of 3D structures in silicon *Sensors Actuators* A **61** 369–73

[10] Bischoff L, Schmidt B, Lange H and Donzev D 2009 Nano-structures for sensors on SOI by writing FIB implantation and subsequent anisotropic wet chemical etching *Nucl. Instrum. Methods* B **267** 1372–5

[11] Elwenspoek M and Jansen H V 1998 *Silicon Micromachining* (Cambridge: Cambridge University Press)

[12] Bai D-J, Zhang Y-Q, Matsushita A, Baba A, Kenjo A, Sadoh T, Nakashima H, Mori H and Tsurushima T 1999 Silicon fine structure formation on sapphire with focused ion beam *Proc. Int. Conf. Ion Implantation (Kyoto)* vol 2 (Piscataway, NJ: IEEE) pp 1101–4

[13] Masahara M *et al* 2004 Ultrathin channel vertical DG MOSFET fabricated by using ion-bombardment-retarded etching *IEEE. Trans. Electron Devices* **51** 2078–85

[14] Ziegler J F and Biersack J P 2008 *SRIM—The Stopping and Range of Ions in Matter* http://www.srim.org/

[15] Franssila S 2004 *Introduction to Microfabrication* (Chichester: Wiley)

[16] Schmidt B, Oswald S and Bischoff L 2005 Etch rate retardation of Ga^+-ion beam-irradiated silicon *J. Electrochem. Soc.* **152** G875–9

[17] Merlos A, Acero M, Bao H, Bausells J and Esteve J 1993 TMAH/IPA anisotropic etching characteristics *Sensors Actuators* A **37/38** 737–43

[18] Resnik D, Vrtacnik D, Aljancic U, Mozek M and Amon S 2005 The role of Triton surfactant in anisotropic etching of {110} reflective planes on (100) silicon *J. Micromech. Microeng.* **15** 1174–83